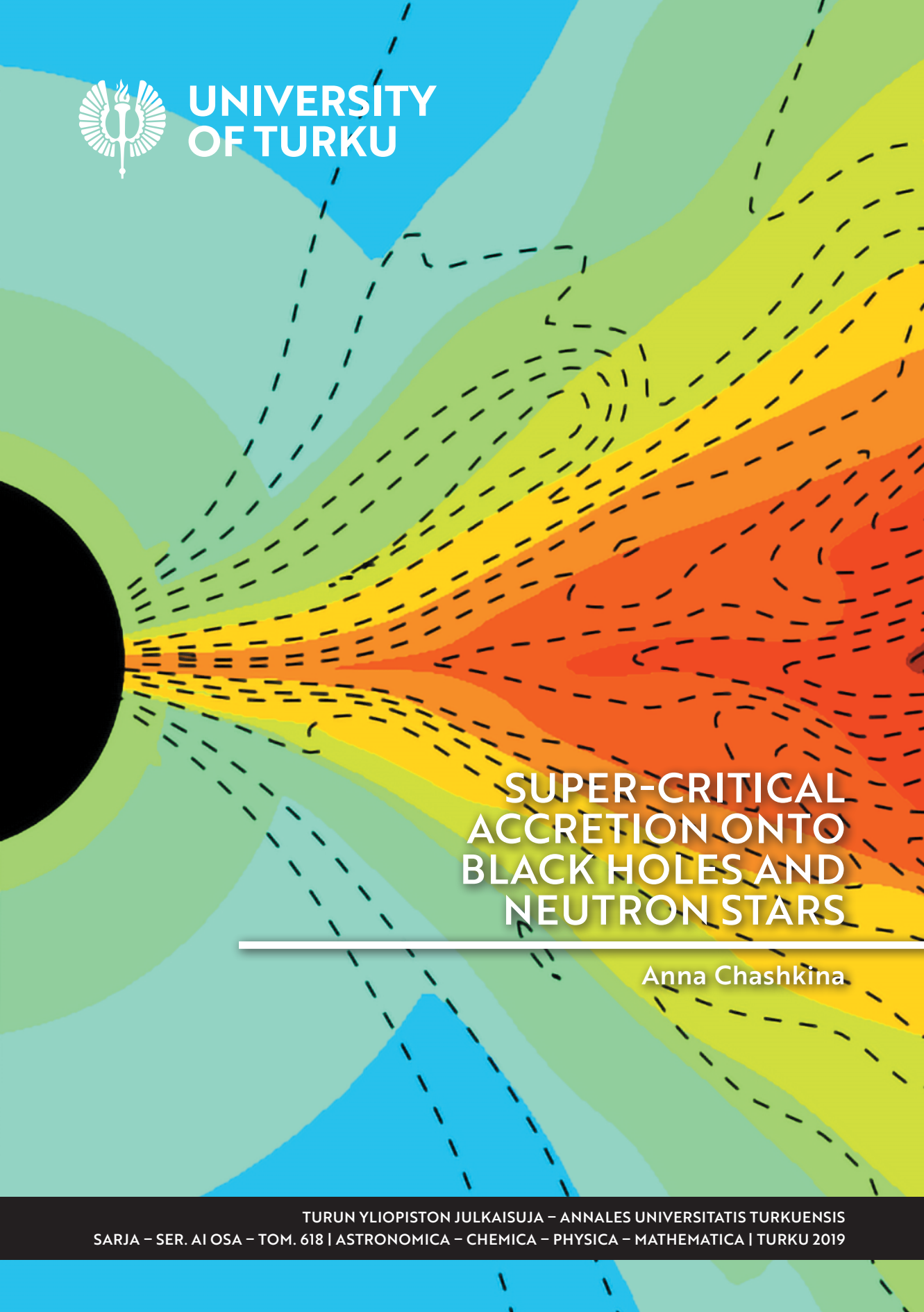

UNIVERSITY OF TURKU

SUPER-CRITICAL ACCRETION ONTO BLACK HOLES AND NEUTRON STARS

Anna Chashkina

TURUN YLIOPISTON JULKAISUJA – ANNALES UNIVERSITATIS TURKUENSIS
SARJA – SER. AI OSA – TOM. 618 | ASTRONOMICA – CHEMICA – PHYSICA – MATHEMATICA | TURKU 2019

UNIVERSITY OF TURKU

SUPER-CRITICAL ACCRETION ONTO BLACK HOLES AND NEUTRON STARS

Anna Chashkina

TURUN YLIOPISTON JULKAISUJA – ANNALES UNIVERSITATIS TURKUENSIS
SARJA - SER. A I OSA - TOM. 618 | ASTRONOMICA - CHEMICA - PHYSICA - MATHEMATICA | TURKU 2019

University of Turku

Faculty of Science and Engineering
Department of Physics and Astronomy

Supervised by

Prof. Juri Poutanen
Tuorla Observatory
University of Turku
Finland

Docent Sergey Tsygankov
Tuorla Observatory
University of Turku
Finland

Reviewed by

Prof. Alexander Tchekhovskoy
Department of Physics and Astronomy
Northwestern University
USA

Prof. Philip Armitage
Department of Physics and Astronomy
Stony Brook University
USA

Opponent

Prof. Włodek Kluźniak
Nicolaus Copernicus Astronomical Center
Polish Academy of Sciences
Poland

The originality of this publication has been checked in accordance with the University of Turku quality assurance system using the Turnitin OriginalityCheck service.

Cover Image: Author

ISBN 978-951-29-7788-8 (PRINT)
ISBN 978-951-29-7789-5 (PDF)
ISSN 0082-7002 (PRINT)
ISSN 2343-3175 (ONLINE)
Painosalama Oy, Turku, Finalnd 2019

LIST OF PUBLICATIONS

Paper I. Abolmasov, P., Chashkina, A.: *On the Eddington limit for relativistic accretion disks*, 2015, Monthly Notices of the Royal Astronomical Society, Volume 454, Issue 4, p.3432-3444, https://doi.org/10.1093/mnras/stv2229

Paper II. Chashkina, A., Abolmasov, P. and Poutanen, J.: *Super-Eddington accretion onto a magnetized neutron star*, 2017, Monthly Notices of the Royal Astronomical Society, Volume 470, Issue 3, p.2799-2813, https://doi.org/10.1093/mnras/stx1372

Paper III. Chashkina, A., Lipunova, G., Abolmasov, P., Poutanen, J.: *Super-Eddington accretion discs with advection and outflows around magnetized neutron stars,* 2019, Astronomy and Astrophysics Volume 626, A18, https://doi.org/10.1051/0004-6361/201834414

PUBLICATIONS NOT INCLUDED IN THE THESIS

I. Chashkina, A., Popov, S.B.: *Magnetic field estimates for accreting neutron stars in massive binary systems and models of magnetic field decay*, 2012, New Astronomy, Volume 17, Issue 6, p.594-602, https://doi.org/10.1016/j.newast.2012.01.004

II. Chashkina, A., and Abolmasov P.: *Black Hole Spin Evolution Affected by Magnetic Field Decay*, 2015, Monthly Notices of the Royal Astronomical Society, Volume 446, Issue 2, p.1829-1847, https://doi.org/10.1093/mnras/stu2078

III. Chashkina, A., Abolmasov, P., Biryukov, A., and Shakura, N.: *Superorbital variability of the X-ray flux in the Be-donor binaries SXP 138, GX-304, and gamma Cas*, 2015, Astronomy Reports, Volume 59, Issue 6, pp.563-572, https://doi.org/10.1134/S1063772915060074

IV. Abolmasov, P., Shakura, N., Chashkina, A.: *Structure of Accretion Discs in Lensed QSOs*, 2018, Accretion Flows in Astrophysics, Astrophysics and Space Science Library, Volume 454. ISBN 978-3-319-93008-4. Springer International Publishing AG, part of Springer Nature, 2018, p. 201, https://doi.org/10.1007/978-3-319-93009-15

Abstract

Accretion is one of the most important processes in astrophysics. Accretion discs are observed in a very large wavelength range, from infrared to X-rays, and in a very large range of scales: from several kilometers (accretion onto a neutron star) to parsecs (gas tori in active galactic nuclei). Physics of accretion discs is diverse, but the basic equations, equations of magnetohydrodynamics, remain the same.

Accretion can also be a radiatively efficient process. As a consequence, radiation pressure easily becomes dynamically important, and a large number of accreting sources exceed their Eddington limit – the luminosity limit beyond which radiation pressure is sufficient to destroy the accretion flow itself.

Ultraluminous X-ray sources (ULXs) are extragalactic non-nuclear sources with huge luminosities $L >$ few $\times 10^{39}$ erg s^{-1} exceeding the Eddington luminosity limits for a stellar mass black hole. Though studied for already about 30 years, they remain interesting both as an extreme case of accreting sources and as an outcome of violent and poorly understood stellar evolution. Besides, recent discoveries have shown many ULXs to contain neutron stars with strong magnetic fields, making them even more extreme both in the sense of fundamental physics and from the point of view of the luminosity excess over the Eddington limit. To meaningfully interpret ULX observations, detailed models of super-Eddington accretion onto compact objects, both of the accretion disc and of the disc-magnetosphere interaction, are highly desirable. However, theoretical models describing accretion at such high rates are complicated by the dominance of radiation pressure, the need to account for advection of energy towards the compact object, and the possible presence of powerful outflows.

We have started our studies by deriving the critical luminosity for a disc around a black hole taking into account disc finite thickness, heat advection, and general relativity (GR) effects. GR effectively makes vertical gravity stronger, and so does inward heat advection. At the same time, normally ignored non-linear vertical gravity dependence on height in a thick disc slightly lowers the limit, resulting in an overall correction by about a factor of two with respect to the classical approach. More accurate result surprisingly depends on the two-dimensional rotation profile of the disc.

For the case of a neutron star with a strong magnetic field, the structure of the disc is not that important by itself as it is essentially invisible and unimportant for the energy budget. However, the position of the disc-magnetosphere boundary is the most important link between the fundamental parameters of the system (magnetic moment of the star, mass accretion rate, viscosity parameter etc.) and the observables (such as spin period and its derivative, power density spectrum of the variability of the source). We developed a model of an accretion disc

around a neutron star taking into account the effects of advection and wind. This model may be applied to a large variety of magnetized neutron stars accreting close to or above their Eddington limits: ULX pulsars, Be/X-ray binaries in outbursts, and other systems.

TIIVISTELMÄ

Massan kertyminen painovoimakentässä on yksi tärkeimmistä astrofysiikan prosesseista. Kertymäkiekkoja voidaan havaita laajalla aallonpituusalueella aina infrapunasta röntgensäteisiin, ja useissa kokoluokissa useista kilometreistä (kertyminen neutronitähdelle) parsekeihin (aktiivisten galaksiydinten kaasurenkaat). Kertymäkiekkojen fysiikka on monipuolista, mutta perusyhtälöt eli magnetohydrodynamiikan yhtälöt pysyvät samoina.

Massan kertyminen voi myös olla säteilyllisesti tehokas prosessi. Tämän seurauksena säteilypaineesta tulee helposti dynaamisesti tärkeä, ja moni kerryttävistä kohteista ylittää Eddingtonin rajansa, luminositeettiraja, jota kirkkaammissa kohteissa säteilyn paine estää massan kertymisen.

Ylikirkkaat röntgenkohteet (ultraluminous X-ray sources, ULX:t), ovat galaksin ulkopuolisia kohteita, joiden huimat luminositeetit $L >$ few $\times 10^{39}$ erg s^{-1} ylittävät Eddingtonin luminositeetit tähdenmassaiselle mustalle aukolle. Vaikka kohteita on tutkittu jo noin 30 vuotta, ne ovat edelleen kiinnostavia äärimmäisiä massaa kerryttäviä kohteita ja rajun sekä huonosti ymmärretyn tähtien elinkaaren lopputuloksia. Viimeaikaiset havainnot osoittavat usean ULX:n sisältävän voimakkaasti magneettisen neutronitähden, mikä tekee niistä entistäkin äärimmäisempiä sekä perustavanlaatuisen fysiikan että Eddingtonin rajan ylittävän kirkkauden näkökulmasta. ULX-havaintojen ymmärtäminen edellyttääkin yksityiskohtaisia malleja Eddingtonin rajan ylittävälle massan kertymiselle, sekä kertymäkiekon että kiekon ja magnetosfäärin vuorovaikutuksen suhteen. Suurilla massankertymismäärillä säteilypaineen dominoiva rooli, tarve ottaa huomioon energian advektio kompaktista kohdetta kohti ja mahdolliset voimakkaat ulosvirtaukset kuitenkin monimutkaistavat teoreettisia malleja.

Olemme aloittaneet tutkimuksemme johtamalla kriittisen luminositeetin mustaa aukkoa ympäröivälle kiekolle ottaen huomioon kiekon rajatun paksuuden, lämmön advektion ja yleisen suhteellisuusteorian (general relativity, GR) vaikutukset. Käytännössä GR voimistaa pystysuuntaista painovoimaa, kuten myös lämmön advektio sisäänpäin. Samaan aikaan, tavallisesti huomiotta jätetty epälineaarinen pystysuuntainen painovoiman riippuvuus korkeudesta paksussa kiekossa hieman alentaa rajaa johtaen kaiken kaikkiaan kahden kokoluokkaa olevaan korjaukseen klassiseen verrattuna. Tarkempi tulos yllättäen riippuu kiekon kaksiulotteisesta pyörimisprofiilista.

Voimakkaasti magnetisoidun neutronitähden tapauksessa kiekon rakenne ei ole niin tärkeä itsessään, sillä se on käytännössä piilossa ja merkityksetön energiabudjetille. Kiekon ja magnetosfäärin rajan sijainti on kuitenkin tärkein linkki järjestelmän perustavanlaatuisten parametrien (tähden magneettinen momentti, massan kertymismäärä, viskositeetti, jne.) ja havaittavien suureiden välillä (mm. pyörimisaika ja sen derivaatta sekä kohteen kirkkauden muutoksen

tehospektri).

Kehitimme neutronitähden kertymäkiekon mallin ottaen huomioon advektion ja tuulen vaikutukset. Tätä mallia voi soveltaa lukuisiin erityyppisiin magneettisiin neutronitähtiin, jotka kerryttävät massaa lähellä tai yli niiden Eddingtonin rajan: ULX-pulsarit, Be-/röntgenkaksoistähdet purkauksissa ja muut järjestelmät.

ACKNOWLEDGEMENTS

Undertaking this PhD has been a truly life-changing experience for me, and it would not have been possible to do without the support and guidance that I received from many people.

First and foremost I want to thank my thesis supervisor Prof. Juri Poutanen for the opportunity to work in his group, for his continuous support of my PhD study, and for his patience. His guidance helped me all the time of research, and in writing this thesis in particular.

I gratefully acknowledge Prof. Alexander Tchekhovskoy and Prof. Philip Armitage for their pre-examination of this thesis, for their insightful comments and encouragement. For sharing with me their immense knowledge and excitement with science. I would also like to thank Prof. Włodek Kluźniak for agreeing to become my esteemed opponent.

My thanks also go out to the support I received from the collaborative work I undertook with Sternberg Astronomical Institute. I am especially grateful to Dr. Galina Lipunova and Prof. Nikolay Shakura. In particular, I am grateful to Prof. Sergei Popov for introducing me to science and showing all its beauty.

My deep appreciation goes out to the high energy astrophysics group of University of Turku members: Sergei Tsygankov, Alexandra Veledina, Andrei Berdyugin, Ilia Kosenkov, Joonas Nättilä, Tuomo Salmi, Juhani Mönkkönen, Vlad Loktev, Vadim Kravtsov, and Armin Nabizadeh.

A very special thank to Pavel Abolmasov for the stimulating discussions, for the sleepless nights we were working together before deadlines, and for all the fun we have had in the last five years.

I would also like to extend my thanks to the people with whom we organize the School of Modern Astrophysics: Vasily Beskin, Alexander Philippov, and Sasha Chernoglasov. For several years, they have been a source of inspiration for me.

I am indebted to all my friends Anton Biryukov, Maria Bogdanova, Ksenia and Slava Zhuravlev, Michael Yurik, Konstantin Petrov, and RTG team.

I gratefully acknowledge the funding sources that made my PhD work possible. I was funded by the Center for International Mobility for my first year, the Väisälä Foundation for the years 2-4.

Lastly, I would like to thank my family for all their love and encouragement. My parents who raised me with a love of science and supported me in all my pursuits. Thank you.

TABLE OF CONTENTS

CHAPTER 1

INTRODUCTION

One of the most powerful processes in the Universe is accretion, infall of gas into a gravitation well. While the efficiency[1] of hydrogen fusion is about 7×10^{-3}, the efficiency of accretion can around be 0.2 for a neutron star (NS) with typical mass $M = 1.4\ \mathrm{M}_\odot$ and radius $R_* = 10$ km, and up to 0.42 for an extremely rapidly rotating Kerr black hole (BH). From the Stefan-Boltzmann's law, the characteristic effective temperature during accretion onto a NS is $T_{\rm eff} \sim 1$ keV, that corresponds to the standard X-ray range. X-ray radiation from an accreting source was first detected in 1962 by a team lead by Riccardo Giacconi [26]. This source, Scorpius X-1, is a NS whose intense gravity draws material off this companion into an accretion disc, from where it ultimately falls onto the surface, releasing a tremendous amount of energy. X-ray radiation from an accreting stellar-mass BH was first detected from the high-mass X-ray binary Cygnus X-1 in 1964 by a sub-orbital rocket experiment [18].

The nature of X-ray sources was unclear at that time. Some of the soft X-ray sources were identified as supernova remnants. Detection of fast variability from X-ray sources helped understand that these objects are very compact, and accretion by a compact source is a plausible explanation for their activity. First works on accretion theory appeared just after the discoveries [27, 59]. The basics of accretion theory was developed in [58], [76], [65], [66] and [44]. Accreting matter may come from the interstellar medium or from a companion star. There are a few possible configurations of an accretion flow: spherical (practically unrealistic), Bondi-

[1] We define efficiency as energy released per unit rest energy $\eta = \dfrac{E}{mc^2} = \dfrac{GM}{Rc^2}$.

Hoyle (axisymmetrical accretion onto a moving compact object), disc, and channelled by magnetosphere.

When matter has insignificant angular and linear momentum, it falls down onto the compact object as a spherical envelope. This regime is known as Bondi accretion [17]. A more realistic case when the compact object moves through a uniform gas cloud is Bondi-Hoyle accretion [30, 21]. This is relevant for the case of the captured stellar wind from a massive donor star in a close binary system. Bondi-Hoyle model fairly describes the accretion flow in such a system in a certain range of radii where the influence of the angular momentum is negligible.

The impact of angular momentum can be illustrated by considering the free-fall case when the matter feels the accretor only through its gravitational field. During the free fall, the matter captured by the gravitational field of the compact object conserves its angular momentum. When the net angular momentum becomes comparable to the local Keplerian value, the radial motion slows down and ultimately seizes when the local Keplerian velocity is exceeded by a factor of $\sqrt{2}$. In order to determine whether matter forms a disc or not at some distance R, we should compare its net angular momentum with the Keplerian angular momentum at this radius $(GMR)^{1/2}$ [33].

During accretion, some fraction of the rest energy is converted to heat and then released as radiation. Accretion luminosity depends on the mass accretion rate $\dot{M}$ as

$$L \simeq \frac{GM\dot{M}}{R}. \tag{1.1}$$

In the spherically symmetric case, there is a luminosity limit for a steadily accreting object, known as the Eddington luminosity [20]. To understand the physical meaning of this limit, let us consider a particle of the mass m affected by two forces, gravity and radiation pressure force. When these two forces balance, matter can not move toward the compact object any more, and

$$\frac{GmM}{R^2} = \frac{L_{\rm Edd}\sigma_T}{4\pi R^2 c}, \tag{1.2}$$

where $\sigma_{\rm T}$ is the extinction cross-section we will hereafter identify with Thomson electron scattering cross-section. The Eddington luminosity for a pure hydrogen plasma is:

$$L_{\rm Edd} = \frac{4\pi GMm_{\rm p}c}{\sigma_T} \simeq 1.3\times10^{38}(M/M_\odot)\,{\rm erg\,s^{-1}}, \tag{1.3}$$

where $m_{\rm p}$ is proton mass. Above the limit, matter is expelled by the radiation pressure in continuum, and accretion seemingly becomes impossible. Any source exceeding this limit for its estimated or expected mass is thus of extreme interest, as it has supposedly found a way to overcome its Eddington limit. There are several hundreds of such sources observed in

Table 1.1: Observational properties of the ULXP.

Name	$L_{\rm X}^{\rm max}$, erg s^{-1}	$P_{\rm s}$, s	$P_{\rm orb}$, d	$\dot{P}_{\rm secular}$, s s^{-1}	References
M82 X-2	2×10^{40}	1.37	2.5	-2.73×10^{-10}	[9]
NGC 7793 P13	2×10^{39}	0.42	3 – 7	-4×10^{-11}	[35, 23, 31]
NGC 5907	10^{41}	1.1	5.3	-8.1×10^{-10}	[34]
NGC 300 ULX 1	5×10^{39}	16		-5.56×10^{-7}	[19, 73]

Observational properties of the known ULXP: maximal luminosity, spin period, orbital period, secular period derivation.

other galaxies, exceeding the Eddington limit for a 10-100 $M_\odot$ black hole. Such objects are known as ultraluminous X-ray sources (ULXs). It is believed that most of these objects are X-ray binaries powered by accretion onto a compact object. Now we know about 500 [74] ULX candidates in all types of galaxies. However the nature of the compact objects in ULXs is still unknown. They can be stellar BHs accreting in a super-Eddington regime [13], or they can be microblazars – sub-Eddington sources with a jet pointing at us [40]. Alternatively, ULXs can be intermediate-mass BHs with masses about $10^3 M_\odot$ [46] or young rotation-powered pulsars [45].

Recently it was realized that some of the ULXs in the nearby galaxies are actually magnetized NSs accreting well above their Eddington limits. Bachetti et al. [9] using *NuSTAR* data discovered coherent pulsations with period of $P \simeq 1.37$ s from the ULX pulsar (ULXP) X-2 in the galaxy M82, see Fig. 1.1. The maximum luminosity of this object is $L \simeq 10^{40}$ erg s^{-1}. This X-ray binary consists of a magnetized NS and a donor star of about $5.2 M_\odot$. The X-ray pulsar spins up at a rate of $\dot{P} \simeq -2 \times 10^{-10}$ s s^{-1}. The source is observed in two states: high, with a luminosity $L \sim 10^{40}$ erg s^{-1}, and low, with a luminosity $L \sim 10^{38}$ erg s^{-1}, see Fig. 1.2. There are no observations showing intermediate luminosities. This behaviour was explained as accretion modulation with the centrifugal barrier set by the rotating magnetosphere of the NS [70]. This transition occurs when the inner parts of the accretion disc rotate at the angular frequency of the NS. The radius of the inner edge of the accretion disc depends on the magnetic field of the NS and the mass accretion rate (see Chapter 3 for the details), this helps estimate the magnetic field of the pulsar in M82 X-2. It was estimated as about 10^{14} G that is comparable to the magnetic fields of magnetars.

Another ULXP, NGC 5907 discovered in [34], broke the luminosity record among the ULXPs (it has $L \sim 10^{41}$ erg s^{-1}), and also shows strong spin-up, $\dot{P} = -5 \times 10^{-9}$ s s^{-1}. Today we already know four ULXPs with $L > 2 \times 10^{39}$ erg s^{-1}. The properties of these sources are listed in Table 1.

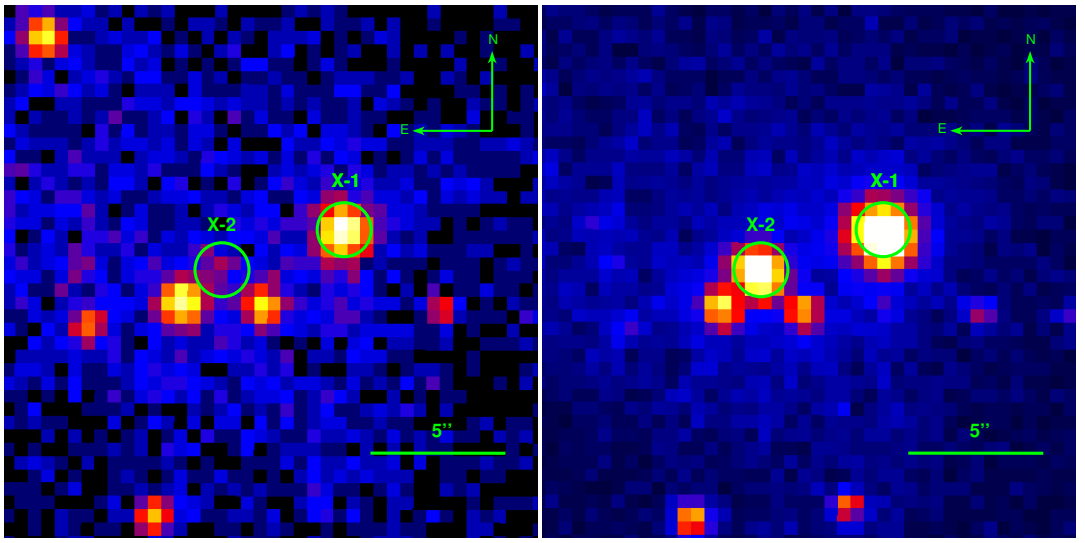

Figure 1.1: Chandra image of the centre of the galaxy M82. The circles indicate the positions of ULXs M82 X-1 and X-2, from [70]. Left panel: ULXP in low state. Right panel: ULXP in high state.

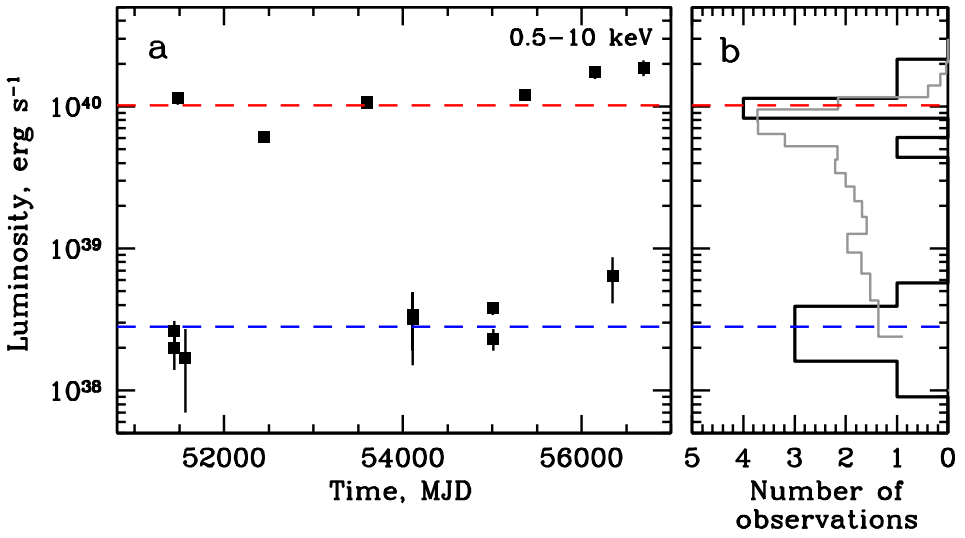

Figure 1.2: (a) Light curve of M82 X-2 obtained by the *Chandra* observatory during 15 years of observations. Luminosities are given for the energy range 0.5 – 10 keV; (b) Distribution of individual observations over luminosities (black line). Bimodal structure is clearly seen. Red and blue dashed lines show the averaged luminosities in the "high" and "low" states, respectively. The grey line represents a rescaled version of the luminosity distribution of the X-ray pulsar LMC X-4 from the Swift/BAT data. From [70].

The discovery of pulsations in M82 X-2 has started the era of ULX pulsars. Many interesting questions arise such as how to explain the excess over Eddington luminosity by a factor of 10-100 observed in many ULXs? What are the magnetic fields in these objects? How does the radiation released close to the NS affect the accretion disc?

In this thesis I consider super-critical accretion onto NSs and BHs. The main issues I address are:

- the possible applications of the standard disc theory to objects exceeding the Eddington limit. In particular, the accretion discs in most ULXPs are large enough to consider them thin, as we do in Paper II.

- The limitations of the applicability of this theory and transition to the supercritical regime. Eddington limit (equation 1.3) was derived for spherically symmetrical accretion. Disc geometry differs from spherical, and Eddington limit in this case will be larger than equation (1.3). Other effects like advection, general relativity effects will change the limit as well. In Paper I we study how different effects change the Eddington limit. As the Eddington limit restricts the maximal amount of mass gain by a compact object, predicting its actual value is of primary importance.

- Contributions of different effects. There are few assumptions in the standard disc theory [66], see Chapter 2. When approaching the Eddington limit these assumptions do not work any more and theory becomes more complicated. There is no analytical model that takes into account all the effects of super-Eddington accretion regime. That is why it is important to understand which effects are more important and how they change the structure of an accretion disc. Contribution of different effects was studied in Paper I.

- Linking theoretical predictions to the observational properties of the real ULXPs. There is still little understanding in how a supercritically accreting NS works. That is why it is important to consider such objects both from theoretical and simulation points of view. In Papers II and III we develop a simple semi-analytical theory that can explain some of the observational properties of ULXPs such as apparently high magnetic fields or spin-up behaviour during outbursts.

Super-critical accretion is one of the most interesting and complicated processes in astrophysics. It causes the most violent periods in the life of NSs and BHs. This is a unique case when the role of radiation pressure forces is comparable to that of gravity, and radiation plays an active role in the dynamics of accreting matter. Evidently, super-Eddington objects are bright, that allows to study them at relatively large distances. In particular, ULXs, unlike fainter

X-ray binaries, are easily observed in nearby galaxies. At the same time, super-Eddington accretion marks the episodes of the most violent evolution in the life of any accreting object, including a SMBH or a stellar-mass BH or a NS in a binary system. Observations of the most distant quasars [42] suggest that SMBH gained their masses through supercritical accretion events. The numerous enigmatic properties of microquasars in general [57] and SS433 [22] in particular suggest an important role that rapid accretion plays in black-hole binary system. And, most importantly, ULXPs, apparently exceeding their Eddington luminosities by a factors of hundreds to thousands, make a new challenge for theorists and modelists who now need to understand which processes may be responsible for the apparently huge luminosities of the accreting NSs.

CHAPTER 2

ACCRETION DISC THEORY

2.1 Basic equations

Almost all the matter in the Universe is in rotation. It can be orbital rotation or rotation in the galaxy. That is why accretion discs are everywhere. In this chapter I will discuss the general theory of accretion discs.

The main equations are the equations of hydrodynamics: continuity, momentum, and energy conservation equations. The continuity equation for a gas with mass density ρ and velocity field $\mathbf{v}$ is

$$\frac{\partial \rho}{\partial t} + \nabla \cdot (\rho \mathbf{v}) = 0. \tag{2.1}$$

The momentum conservation (Euler equation with an additional viscous term on the RHS) has the form:

$$\rho \frac{\partial \mathbf{v}}{\partial t} + \rho(\mathbf{v} \cdot \nabla)\mathbf{v} = -\nabla P - \rho \nabla \Phi + \nabla \overleftrightarrow{w}. \tag{2.2}$$

The pressure gradient ∇P is important in the vertical direction, Φ is the gravitational potential, $\overleftrightarrow{w}$ is the viscous stress tensor, it transfers the momentum along velocity gradients from the inner parts of the disc to its outer parts. The important component of it is $\mathrm{w}_{r\varphi}$, responsible for angular momentum transfer. The second term on the LHS is advection of momentum. In the frame corotating with the disc it can be written as $(\mathbf{v} \cdot \nabla)\mathbf{v} = (\mathbf{v}_\mathrm{p} \nabla)\mathbf{v}_\mathrm{p} + \Omega^2 \mathbf{R}$, where $\Omega = v_\varphi / R$

is angular velocity at a given radius R, and $\mathbf{v}_\mathrm{p}$ is poloidal velocity (we will assume the velocity composed of toroidal (azimuthal) and poloidal components and $v_\mathrm{p} \ll v_\varphi$).

The third equation of the main system of equations is the energy balance:

$$Q_+ = Q_\mathrm{rad} + Q_\mathrm{adv}, \tag{2.3}$$

where Q_+ is the amount of heat generated by viscosity per unit area, Q_rad is radiative cooling rate, and Q_adv is heating or cooling rate by advection. We assume Q_adv to be positive if the heat is advected inwards.

The radiative cooling rate from the both sides of the disc may be expressed in terms of effective temperature T_eff:

$$Q_\mathrm{rad} = 2\sigma_\mathrm{SB} T_\mathrm{eff}^4, \tag{2.4}$$

where σ_SB is Stefan-Boltzmann's constant and T_eff is effective temperature. The advected flux Q_adv may be viewed (as it is done, for instance, in [43]) as the flux of heat carried with the flow, and thus may be expressed through the specific entropy per particle s

$$Q_\mathrm{adv} = \int_{-H}^{H} \rho v_r \frac{kT}{\tilde{m}} \frac{\mathrm{d}s}{\mathrm{d}R} \mathrm{d}z\,, \tag{2.5}$$

where v_r is the radial velocity, H is disc thickness, and $\tilde{m}$ is the mean particle mass.

The energy dissipating per unit time per unit volume is [41]

$$q_+ = w_{ik} \frac{\partial v_i}{\partial x_k}. \tag{2.6}$$

In Newtonian viscosity approach it can be written as:

$$q_+ = \rho \nu r^2 \left(\frac{\mathrm{d}\Omega}{\mathrm{d}R}\right)^2, \tag{2.7}$$

where ν is Newtonian kinematic viscosity. The total energy released in the disc per unit area is:

$$Q_+ = \int_{-H}^{H} q_+ \mathrm{d}z. \tag{2.8}$$

Kinematic viscosity was shown to be inefficient in most of the accreting sources [51]. However there are different mechanisms in accretion discs capable of acting as viscosity, including spiral waves [8, 10] and magneto-hydrodynamic turbulence excited by instability mechanisms like the magneto-rotational instability [11]. The simplest way to describe viscosity in the disc is to assume that viscous stresses are proportional to the pressure in the disc with some coefficient $0 < \alpha < 1$ [66]:

$$w_{r\varphi} = \alpha P. \tag{2.9}$$

Viscous stresses may be due to magnetic fields or turbulence. In both cases, the constancy of α is ensured by equipartition understood as proportionality between the energy density of magnetic fields or turbulent motions and the thermal energy density. Thus, the turbulent component of the dimensionless viscosity parameter can be estimated as the mean turbulent Mach number[1] squared, $\alpha_t \sim \langle M_t^2 \rangle$. This α prescription was introduced by [66] and now widely used. From observations $\alpha = 0.1..1$ [37] but simulations generally predict smaller values $\alpha \sim 0.01$ [56].

2.2 Steady thin disc

The main assumptions of the standard accretion disc theory are:

- axially symmetric and stationary disc,
- small geometric thickness of the disc (which allows to separate variables in the dynamic equations, calculating independently the vertical and the radial structure),
- all the other velocity components are small in comparison with v_φ; radial velocity is used only in the equation for angular momentum transfer,
- the vertical optical depth of the disc is large,
- there is no substantial heat transfer in the radial direction,
- the vertically integrated component of the viscous stress tensor $W_{r\varphi} = \int_{-H}^{H} w_{r\varphi} \mathrm{d}z$ is proportional to the pressure of the disc integrated over vertical direction $\Pi = \int_{-H}^{H} P \mathrm{d}z$: $W_{r\varphi} = \alpha\Pi$, where α is a dimensionless constant normally smaller than unity and H is the half-thickness of the disc,
- the boundary condition in the case of accretion onto a BH is: $W_{r\varphi} = 0$ at the inner radius.

Let us write the main equations describing the disc in these assumptions. The continuity equation is:

$$\frac{1}{R}\frac{\partial}{\partial R}(\Sigma v_r R) = 0, \tag{2.10}$$

which in the integral form corresponds to a constant mass accretion rate $\dot{M} = -2\pi\Sigma v_r R$.

[1] we define the turbulent Mach number as the mean turbulent motion velocity in the units of the speed of sound.

The momentum equation (2.2) in z-direction is in our assumptions reduced to hydrostatics

$$0 = -\frac{1}{\rho}\frac{\mathrm{d}P}{\mathrm{d}z} - \frac{GM}{R^3}z. \tag{2.11}$$

$|\partial P/\partial z|$ can be approximated by P/H that implies

$$\frac{1}{\rho}\frac{P}{H} \simeq \Omega_{\mathrm{K}}^2 H, \tag{2.12}$$

where $\Omega_{\mathrm{K}} = \sqrt{\frac{GM}{R^3}}$. If the sound speed is $c_{\mathrm{s}} \simeq \sqrt{P/\rho}$, disc thickness becomes

$$H \simeq \frac{c_s}{\Omega_{\mathrm{K}}}. \tag{2.13}$$

Radial component of momentum equation (2.2) becomes

$$v_r\frac{\partial v_r}{\partial R} + v_z\frac{\partial v_r}{\partial z} - \Omega^2 R = -\frac{1}{\rho}\frac{\partial P}{\partial R} - \frac{GM}{R^2}. \tag{2.14}$$

In the thin-disc approximation we can neglect the first and the second terms in the LHS as well as well as the pressure gradient in the RHS, because they are small. From the radial angular momentum transfer and from the vertical hydrostatic equilibrium (2.11) we get:

$$\frac{v_{r,z}^2}{R} \sim \left(\alpha\left(\frac{H}{R}\right)^2\right)^2\frac{GM}{R^2}, \tag{2.15}$$

$$\frac{1}{\rho}\frac{\partial P}{\partial R} \sim \left(\frac{H}{R}\right)^2\frac{GM}{R^2}. \tag{2.16}$$

Finally, the radial component of momentum equation (2.14) becomes

$$\Omega^2 R = \frac{GM}{R^2}. \tag{2.17}$$

That ensures Keplerian rotation with $\Omega = \Omega_{\mathrm{K}}$.

The momentum equation in the azimuthal direction is:

$$\Sigma v_r R\frac{\partial(\Omega R^2)}{\partial R} = -\frac{\partial(W_{r\varphi}R^2)}{\partial R}, \tag{2.18}$$

where Σ is surface density $\Sigma = \int_{-H}^{H}\rho\mathrm{d}z$. Integrating this equation we get:

$$\dot{M}\Omega R^2 - 2\pi W_{r\varphi}R^2 = \text{const.} \tag{2.19}$$

The constant can be found from the boundary conditions. The standard thin disc assumes zero boundary condition at its inner edge which corresponds to the innermost stable orbit $R_{\rm in}$ in the case of a BH: $W_{r\varphi}(R_{\rm in}) = 0$. Applying this condition yields

$$\dot{M}\Omega(R)\left(1-\sqrt{\frac{R_{\rm in}}{R}}\right) = 2\pi W_{r\varphi}. \tag{2.20}$$

A nontrivial boundary condition at the inner edge of the disc may arise in case of accretion onto a rapidly rotating compact object with a strong magnetic field.

In order to estimate the viscous stress tensor one can use α-prescription:

$$\mathrm{w}_{r\varphi} = \alpha P, \tag{2.21}$$

where $P = P_{\rm gas} + P_{\rm rad}$ is disc pressure, composed of the gas pressure $P_{\rm gas} = nkT$ and the radiation pressure $P_{\rm rad} = \frac{1}{3}aT^4$ in the disc.

Another conserved quantity is energy. In the standard disc model, there is a local energy balance: all the energy generated by viscosity $Q_+(R)$ is radiated from the surface at the same radius as radiation flux $Q_{\rm rad}(R)$:

$$Q_+ = Q_{\rm rad}. \tag{2.22}$$

Amount of heat generated by viscosity between two of the surfaces of the disc:

$$Q_+ = 2\int_0^H q_+ \mathrm{d}z = -W_{r\varphi}R\frac{\mathrm{d}\Omega}{\mathrm{d}R}. \tag{2.23}$$

For a BH with the trivial boundary condition it is:

$$Q_+ = \frac{3}{4\pi}\dot{M}\Omega_{\rm K}^2\left(1-\sqrt{\frac{R_{\rm in}}{R}}\right). \tag{2.24}$$

In order to estimate $Q_{\rm rad}$, one can use diffusion approximation:

$$\frac{c}{3\kappa\rho}\frac{\mathrm{d}(aT^4)}{\mathrm{d}z} = -F^-, \tag{2.25}$$

where F^- is energy flux, $a = 4\sigma_{\rm SB}/c$ is radiation constant, and κ is the opacity. There are two main sources of opacity: scattering on free electrons (Thomson opacity $\kappa_{\rm es} \simeq 0.34$ cm^2 g^{-1} for solar metallicity) and free-free transitions $\kappa_{\rm ff}$. Radiative cooling rate can be expressed through the surface energy flux as

$$Q_{\rm rad} = 2F^-|_{z=H}. \tag{2.26}$$

At high mass accretion rates, when radiation pressure dominates over $P_{\rm gas}$, the vertical scaleheight of the disc can be obtained by equating the pressure created by vertical radiation flux, $\kappa F^-/c$, and vertical gravity $g_z = GMH/R^3$:

$$\frac{\kappa F^-}{c} = \frac{GM}{R^3} H. \tag{2.27}$$

This equality gives us disc thickness in the radiation-pressure-dominated regime:

$$H = \frac{3}{8\pi}\frac{\kappa \dot{M}}{c}\left(1 - \sqrt{\frac{R_{\rm in}}{R}}\right). \tag{2.28}$$

These equations describe the structure of a standard thin disc. Standard disc model well describes the accretion discs in the systems with luminosities $0.05 L_{\rm Edd} \leq L \leq 0.5 L_{\rm Edd}$. When the luminosity is outside this range, the inner parts of the disc become thick. Both cases, small and large mass accretion rates, are considered in subsection 2.4.

2.3 Relativistic standard disc

The model of standard disc was extended to relativistic case [50]. The main assumptions of this model are:

- the disc plane coincides with the equatorial plane of the BH,
- the companion star in the binary system has negligible gravitational influence on the disc structure (assumption usually valid in the inner parts of disc, where general relativity effects are important),
- the disc is geometrically thin, $H(R) \ll R$,
- the disc is in a quasi-steady state,
- the gas of the disc moves in circular, geodesic orbits.

In this section we will follow the work of [16]. All the equations are in Kerr metric g_{ik} in Boyer-Lindquist coordinates $x^i = (t, r, \theta, \varphi)$:

$$ds^2 = -\left(1 - \frac{2r}{\Sigma^*}\right)dt^2 - \frac{4ar\sin^2\theta}{\Sigma^*}dt d\varphi + \frac{\Sigma^*}{\Delta}dr^2 + \Sigma^* d\theta^2 + \left(r^2 + a^2 + \frac{2ra^2\sin^2\theta}{\Sigma^*}\right)\sin^2\theta d\varphi^2. \tag{2.29}$$

where $r = Rc^2/(GM) = R/R_{\rm g}$, $R_{\rm g} = GM/c^2$ is gravitational radius, $a = Jc/(GM^2)$ is Kerr parameter, $\Delta = r^2 - 2r + a^2$, and $\Sigma^* = r^2 + a^2\cos^2\theta$.

The four-velocity of the accreting gas is $u^i = (u^t, u^r, u^\theta, u^\varphi)$. The angular velocity of the gas is $\Omega = u^\varphi/u^t$, net angular momentum $l = -u_\varphi/u_t$.

Let us write the equations of accretion theory in relativistic form. The equation of baryonic number conservation is

$$\nabla_i(\rho u^i) = 0. \tag{2.30}$$

From here, integrating in vertical direction, we get in the steady state

$$\dot{M} = 2\pi r \Sigma u^r = \text{const}. \tag{2.31}$$

Here, the surface density $\Sigma = \int_{-H}^{H} \rho \mathrm{d}z = \int_0^{2\pi} \rho\sqrt{g_{\theta\theta}}\mathrm{d}\theta$. The additional metric multiplier is $\sqrt{g_{\theta\theta}} \simeq r$ near the equatorial plane.

Similarly, the vertically integrated equations of conservation of energy and angular momentum acquire the form

$$\frac{\partial}{\partial r}\left[\mu\left(\frac{\dot{M}}{2\pi}u_t + 2r\nu\Sigma\sigma^r_t\right)\right] = \frac{Q_{\rm rad}}{c^2}u_t r \tag{2.32}$$

and

$$\frac{\partial}{\partial r}\left[\mu\left(\frac{\dot{M}}{2\pi}u_\varphi + 2r\nu\Sigma\sigma^r_\varphi\right)\right] = \frac{Q_{\rm rad}}{c^2}u_\varphi r, \tag{2.33}$$

where

$$\mu = \frac{E + \Sigma c^2 + \Pi}{\Sigma c^2} \tag{2.34}$$

is relativistic enthalpy, σ^r_ϕ and σ^r_t are non-trivial components of the shear stress tensor, $Q_{\rm rad}$ are radiative losses, E is the vertically integrated internal energy density. Radiative losses $Q_{\rm rad}$ can be written as twice the flux measured in the co-moving reference frame and are the same as in non-relativistic case, see eq. (2.26).

In Navier-Stokes approximation (viscous stress tensor components proportional to the corresponding strain tensor component), non-trivial components of the shear stress tensor are:

$$\sigma^r_\varphi = \frac{1}{2}g^{rr}g_{\varphi\varphi}\sqrt{-g^{tt}}\gamma^3\frac{\mathrm{d}\Omega}{\mathrm{d}r}, \tag{2.35}$$

$$\sigma^r_t = -\Omega\sigma^r_\varphi, \tag{2.36}$$

where $\gamma = u^t(-g^{tt})^{-1/2}$ is Lorentz-factor measured in the frame of local observers having zero angular momentum and Ω is angular velocity.

The radial component of momentum equation in thin-disc approximation can be written as:

$$\frac{1}{2}\frac{\mathrm{d}u^r u_r}{\mathrm{d}r} + \frac{u_r Q_+}{c^3 \Sigma \mu} + \frac{1}{c^2 \Sigma \mu}\frac{\mathrm{d}\Pi}{\mathrm{d}r} - \frac{1}{2}\gamma^2 g^{tt}(\Omega - \Omega_K^-)(\Omega - \Omega_K^+)\frac{\partial g_{\varphi\varphi}}{\partial r} = 0, \tag{2.37}$$

where Keplerian angular velocities for the co-rotating (+) and counter-rotating (-) orbits in relativistic case are: $\Omega_K^{\pm} = \pm\dfrac{1}{r^{3/2} \pm a}$. Surface viscous heating rate in relativistic approach is

$$Q_+ = 2\nu\Sigma\sigma^2 c^2, \tag{2.38}$$

where $\sigma^2 = \dfrac{1}{2} g^{rr} g_{\phi\phi}(-g^{tt})\gamma^4 \left(\dfrac{\mathrm{d}\Omega}{\mathrm{d}r}\right)^2$.

2.4 Thick discs

At low accretion rates, diffusion approximation (eq. 2.25) is not applicable because the disc becomes optically thin. For such a disc, the efficiency of radiation cooling is very low. Thermal energy released in the flow by viscosity is not going to be radiated away, but will be advected towards the compact object. In the case of a BH this advected energy is lost in the hole, in the case of a NS it is thermalized and reradiated from the stellar surface. Such an accretion flow more likely exists in the form of a two-temperature plasma and is cooled by synchrotron, bremsstrahlung, and other processes. This type of accretion regime is called ADAF – advection-dominated accretion flow [32, 48, 49, 4, 5].

For ULXs, more relevant is the opposite case, when $\dot{M}$ is high [14, 3, 1]. Heat generation increases with increasing mass accretion rate $Q_+ \propto \dot{M}$, see eq. (2.23). From the local energy balance eq. (2.22), radiation energy losses increase as well. As radiation pressure is opposed by the vertical gravity (eq. 2.27), thickness of the disc increases.

In the standard disc model, we neglected all the terms $\sim (H/R)^2$, but this cannot be done when $H \sim R$. The first new quantity appearing in the radial dynamic equation (2.14) is the pressure gradient. Disc now rotates with the angular frequency different from Keplerian. The related radius at which the scale height of the disc becomes comparable to its radius is known as the *spherization radius*.

In the model of [66] this distance is $R_{\mathrm{sph}} = 3/2\dot{m}R_{\mathrm{g}}$, where $\dot{m} = \dot{M}c^2/L_{\mathrm{Edd}}$ is dimensionless mass accretion rate. More accurate estimates taking into account the inner boundary condition in the standard theory framework give [2]:

$$R_{\mathrm{sph,\,NR}} = \frac{3}{2}\dot{m}R_{\mathrm{g}} \cdot \frac{4}{3}\cos^2\left(\frac{1}{3}\arccos\left(-\frac{3\sqrt{R_{\mathrm{in}}/R_{\mathrm{g}}}}{\sqrt{2\dot{m}}}\right)\right). \tag{2.39}$$

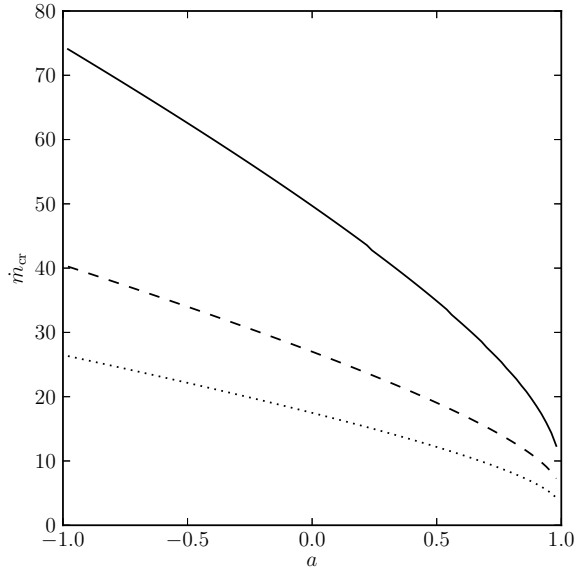

Figure 2.1: Critical mass accretion rate as a function of Kerr parameter a. Dotted line is the critical rate for spherically symmetric accretion, dashed line is the maximal mass accretion rate in Newtonian approximation (eq. 2.39), and the solid line corresponds to the limit in full general relativity (eq. 2.40), see Paper I.

In the model of relativistic standard disc, the spherization radius is found by solving the expression

$$R_{\rm sph} = \frac{3}{2}\dot{m}\frac{\mathscr{Q}(R_{\rm sph},a)}{\mathscr{B}(R_{\rm sph},a)}\frac{\sqrt{\mathscr{C}(R_{\rm sph},a)}}{C_r(R_{\rm sph},a)}R_{\rm g}, \tag{2.40}$$

where calligraphic letters are correction coefficients introduced in the works by [52] and [62]:

$$\mathscr{B} = 1 + \frac{a}{(R/R_{\rm g})^{3/2}}, \tag{2.41}$$

$$\mathscr{C} = 1 - \frac{3}{R/R_{\rm g}} + \frac{2a}{(R/R_{\rm g})^{3/2}}, \tag{2.42}$$

$$\mathscr{Q} = \frac{\mathscr{B}}{\sqrt{r\mathscr{C}}}\left(\sqrt{R/R_{\rm g}} - \sqrt{R_{\rm in}/R_{\rm g}} - \frac{3}{4}a\ln\frac{R}{R_{\rm in}} - A_1 - A_2 - A_3\right), \tag{2.43}$$

A_1, A_2, A_3 are coefficients from [50] and [52]. The critical $\dot{m}$ when the disc starts to achieve $H = R$ at some radius (and equation 2.39 or 2.40 starts having a solution) in non-relativistic and relativistic regimes is shown in Fig. 2.1.

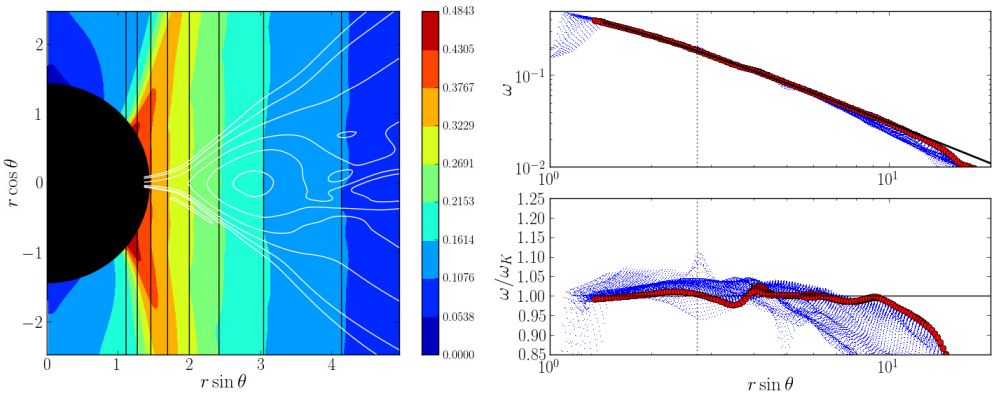

Figure 2.2: Time-averaged density and angular frequency map calculated using a HARM2D simulation. Left panel: colour-coded is angular velocity $\Omega = u^\varphi/u^t$ in c^3/GM units, black lines are vertical (Ω = const) lines corresponding to the same values of angular velocity as the boundaries between different colours/shades. Right panels: angular frequency slice through the equatorial plane (thick red points) and for polar angle $45^\circ \le \theta \le 135^\circ$; solid black line is Keplerian law. Lower right panel shows relative deviations from the cylindrical Keplerian law. All the distances are in R_g units. Vertical dotted lines mark the radius of the last stable orbit. See Paper I for the details.

When the time scale for radial motion and the radiative cooling time are comparable, the local energy balance (eq. 2.22) is broken: a fraction of the energy produced at some radius R_0 is stored in the disc as thermal energy and advected into the black hole instead of being radiated away, the other will be radiated away at some other distance $R < R_0$.

It is hard to describe the structure of a thick disc analytically. Without the thin-disc approximation, it is impossible to separate the variables in the equations, and all the quantities should be solved for in two dimensions simultaneously. Apart from advection effects discussed above, it is also important to take into account the radial pressure gradient. According to the radial Euler equation, significant pressure gradient leads to non-Keplerian rotation in the disc. We need numerical simulations to construct the thick disc. The structure of a simulated thick relativistic disc is shown in Fig. 2.2.

CHAPTER 3

ACCRETION ONTO A NEUTRON STAR

3.1 Introduction

Accretion onto a NS differs from BH accretion in a number of ways. Unlike a BH, NS has a surface, therefore the accreted matter and released energy are not lost below the horizon. Depending on the mass accretion rate, observable X-ray radiation may come predominantly from accretion flows or some heated parts of the surface of the star. The second difference is that NSs have magnetic fields. Presence of magnetic fields disrupts the accretion disc and channels the accreting matter along the field lines. The outcome of the interaction between the magnetic field of the NS and the matter being accreted depends on the properties of the NS.

This interaction is thought to lead to a wide variety of X-ray activity, for instance X-ray pulses, quasi-periodic oscillations, stochastic variability, jets etc. Many of them are attributed to the interaction between accretion flows and the magnetosphere of the star.

Neutron stars may be classified by the energy sources powering their emission and spin evolution [28]. Rotation-powered NSs extract their energy from the rotation of the NS. Most numerous (in the sample of all the observed NSs) class of the rotation-powered NSs are radio pulsars [36]. These objects have a wide range of magnetic field strengths $B = 10^8 - 10^{13}\,\mathrm{G}$ and spin periods from $1.4\,\mathrm{ms}$ [29] to $23.5\,\mathrm{s}$ [68]. Magnetars are a class of magnetically-driven NSs, whose radiation comes from very strong decaying magnetic fields. They are isolated NSs with periods $2 - 12$ s and extremely high magnetic fields $10^{14} - 10^{15}\,\mathrm{G}$ [72].

In my research, I focus on accretion-powered NSs. These NSs reside in binary systems

and accrete matter from a donor star. Accreting NSs display a wide variety of behaviours, depending on the NS magnetic field strength, mass of the companion and properties of the accretion flow. Low-mass X-ray binaries (LMXB) contain low-mass ($\lesssim 1 M_\odot$) donor stars such as brown dwarfs, white dwarfs, red giants, but most likely low-mass main-sequence or sub-giant stars. The donor star fills its Roche lobe, and accretion runs through the inner Lagrangian point forming an accretion disc. NSs in LMXBs are believed to be old and have weak magnetic fields $B \sim 10^8$ G [28]. Because of the small magnetic field, the accretion disc comes close to the surface of the NS, gradually spinning the NS up. Some LMXBs exhibit X-ray bursts that are interpreted as thermonuclear explosions on the surface of the NSs [67].

High mass X-ray binaries (HMXB) consist of NSs and high-mass donor stars $M > 2M_\odot$. The donor star loses mass through a strong spherically symmetric wind or through a decretion disc (in the case of a Be donor star). Stellar wind is then captured by the NS. A large subclass of HMXBs is Be/X-ray binaries [60]. These are mostly wide, eccentric binaries where the accretion rate is strongly modulated with the orbital period, and a large fraction of matter s transported in short flares. The flares are probably related to the the donor Be star losing matter through a decretion disc or a dense equatorial wind. Spin periods of these NSs vary in the range $\sim 1 - 1000$ s, and magnetic fields are about $B \sim 10^{12-14}$ G.

In my thesis I focus on ULXPs which are likely the HMXB accreating via Roche lobe overflow. In order to understand the observational properties of this type of NS, one should introduce some important radii. Let us consider the case when matter moves inward at the free-fall velocity $v_{\rm ff} = \sqrt{\dfrac{2GM}{R}}$. Spherically symmetric inflow ram pressure $\rho v_{\rm ff}^2$ opposes magnetic field pressure $B^2/8\pi$. At some distance $R_{\rm A}$ (*Alfvén radius*), where both pressures are equal, the inward motion stops:

$$R_{\rm A} = \left(\frac{\mu^2}{2\dot{M}\sqrt{2GM}}\right)^{2/7}, \tag{3.1}$$

where $\mu \simeq B_* R_*^3$ is the magnetic moment of the NS of the radius R_*, mass M and dipole magnetic field on its surface B_*.

However, matter can penetrate through the magnetosphere and accrete onto the NS surface because of the instabilities at the magnetospheric boundary, for instance interchange instability [7], or because of the reconnections in the magnetosphere [53]. Persistent accretion is possible if the magnetosphere is rotating slower than the disc at the magnetopsheric boundary. Assuming Keplerian rotation, one can estimate the distance $R_{\rm co}$(*corotation radius*) where the angular

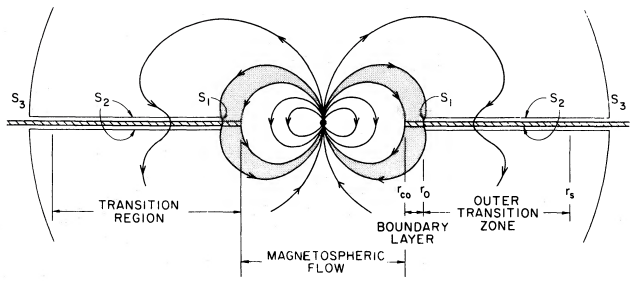

Figure 3.1: Side view of the accretion flow and NS magnetosphere, taken from by [24].

velocity of the magnetic field lines $\Omega_{\rm NS}$ and the disc are the same

$$R_{\rm co} = \left(\frac{GM}{\Omega_{\rm NS}^2}\right)^{1/3}. \tag{3.2}$$

If the magnetosphere rotates faster than the accretion disc, and thus $R_{\rm co} < R_{\rm A}$, centrifugal forces may lead to ejection of the accreting matter (see [33]). This regime is called *propeller*. In this thesis I will primarily consider the case of $R_{\rm co} > R_{\rm A}$ when accretion is possible.

3.2 Magnetospheric accretion

The physical structure and processes acting in the inner regions of accretion discs are still poorly constrained, yet they are the key elements for understanding disc dynamics and evolution. In this region, the interaction between the magnetic field of the NS and the matter of the disc is a key factor controlling the gas accreting onto the NS via magnetic lines. There is still no clear picture of such interaction. One of the classical approaches [25, 24] is to assume that magnetic field of the NS penetrates the disc in a wide range of radii, see Fig. 3.1. Accretion disc rotates according to Keplerian law, hence it has different angular velocities at different radii while magnetic field lines are anchored in the surface of the star and rotate with the NS. This leads to the magnetic field lines being twisted and wound up. In order to maintain such a configuration for a time longer than several spin periods, material of the disc should have very large magnetic diffusivity. As the gas in the disc is mostly ionized, its conductivity is very large, making the effective magnetic diffusivity very low.Despite this evident inconsistency, such an approach is widely used. With some modifications [38, 75] taking into account the finite size of the interaction region, such a model may provide a reasonable physical description for an infinitely thin disc.

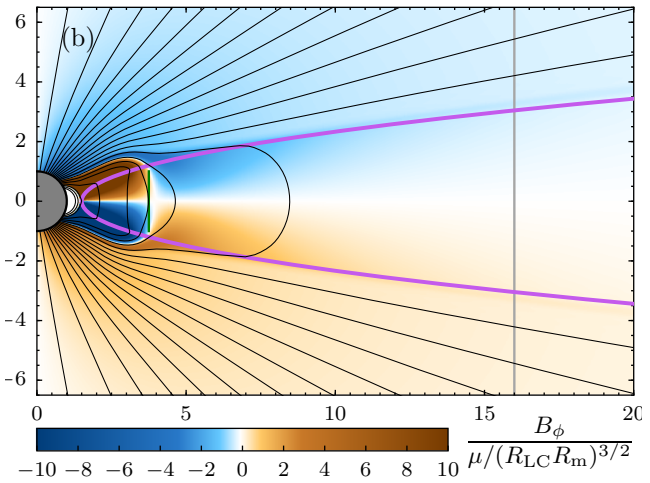

Figure 3.2: Thin infinitely conducting disc simulations by [55]. The axis scales are in units of NS radius. Light cylinder ($R_L = c/\Omega_{\rm NS}$) is shown with a vertical gray line, the short green line indicates the corotation radius in the disc. The outline of the disc is drawn in purple, poloidal field lines are shown in black. The color indicates the toroidal magnetic field.

Another approach is to consider the disc interacting with the stellar magnetic field only in a very narrow region near the inner boundary of the disc, as it was done by [64] and later by [6]. This idea is in good agreement with simulations [63, 54, 55, 53], see Fig. 3.2, if the disc is an idea conductor.

In the Papers II and III, we followed the second approach and reduced the interaction with the magnetosphere to a set of boundary conditions (Paper II). First boundary condition follows from angular momentum conservation

$$\dot{M}_{\rm in}(\Omega_{\rm in} - \Omega_{\rm ns})R_{\rm in}^2 = \kappa_t \frac{\mu^2 H_{\rm in}}{R_{\rm in}^2}, \tag{3.3}$$

where $\dot{M}_{\rm in}$ and $\Omega_{\rm in}$ are the mass accretion rate and the angular velocity at the inner edge of the disc $R_{\rm in}$, $H_{\rm in}$ is the half-thickness of the disc, and the dimensionless constant κ_t parametrizes the efficiency of the angular momentum removal by the magnetic and viscous torques. This condition assumes that, as the matter from the disc enters the magnetosphere and starts corotating with the NS, the excess angular momentum (LHS) is removed by the magnetic stresses at the magnetospheric boundary (RHS). The second boundary condition is the pressure balance combined with α prescription

$$W_{r\phi}^{\rm in} = 2\alpha H_{\rm in} \frac{\mu^2}{8\pi R_{\rm in}^6}. \tag{3.4}$$

Here, internal pressure in the disc is balanced by the external magnetic field pressure, $W_{r\phi}^{in}$ is the vertically integrated rϕ - component of the viscous stress tensor at the inner boundary.

A thin disc structure calculated with these boundary conditions is shown in Fig. 3.3. Here the disc structure with non-trivial boundary conditions is plotted with a red line. Gas-pressure- and radiation-pressure-dominated standard disc models are shown by blue dotted and green dashed lines, respectively. One can see that the deviations from Keplerian rotation are very small. The disc has non-zero thickness at the inner boundary but $(H/R)_{\max}$ is smaller than that for a standard disc because the matter is accumulated near $R_{\rm in}$ and the surface density becomes higher while vertically integrated pressure stays the same.

The disc structure around X-ray pulsars is well approximated by the standard accretion model together with the boundary conditions introduced above. For the magnetic field values inferred for ULXPs, the magnetospheric radii are about hundred times larger than the NS radius. Due to the large magnetosphere size, even a hundred-fold excess of Eddington limit does not mean the accretion disc becomes super-Eddington. When the mass accretion rate becomes high enough for the inner parts of the disc to enter supercritical regime, thin disc approximation is no more valid. Then, it is important to take into account outflows from the disc and advection effects. Super-Eddington disc can exist around ULXP NGC 5907 X-1, that has a maximal luminosity $L \sim 10^{41}$ erg s^{-1}.

In the presence of a wind, the angular momentum conservation equation is modified by an additional term corresponding to the angular momentum outflow in the wind:

$$\frac{\mathrm{d}\left(\dot{M}(R)\Omega R^2\right)}{\mathrm{d}R} = \frac{\mathrm{d}}{\mathrm{d}R}\left(2\pi R^2 W_{r\phi}\right) + \frac{\mathrm{d}\dot{M}(R)}{\mathrm{d}R}\Omega R^2 \psi, \tag{3.5}$$

where $\psi \geq 1$ allows us to scale up the net angular momentum lost in the wind. Large ψ can appear in magneto-centrifugal winds.

It is reasonable to assume that some fraction $\epsilon_{\rm w} \leq 1$ of the energy leaving the disc with radiation is spent to accelerate the outflow [43, 57]:

$$\epsilon_{\rm w} Q_{\rm rad} = \epsilon_{\rm w} 2\sigma_{\rm SB} T_{\rm eff}^4 = \frac{\Omega_{\rm K}^2 R}{4\pi}\frac{\mathrm{d}\dot{M}(R)}{\mathrm{d}R}. \tag{3.6}$$

During magnetospheric accretion, the matter moves along the magnetic field lines onto the magnetic poles of the NS. Depending on the magnetic field strength and mass accretion rate, the matter can form either a hot polar cap or a configuration called accretion column [12]. Most of the radiation in super-Eddington X-ray pulsars is released in the accretion column, the contribution of the accretion disc is only about $R_*/R_{\rm in}$. The accretion disc, at the same time, becomes illuminated by the radiation flux exceeding the local Eddington limit, and thus its structure as well as the position of the disc-magnetosphere interface should be affected

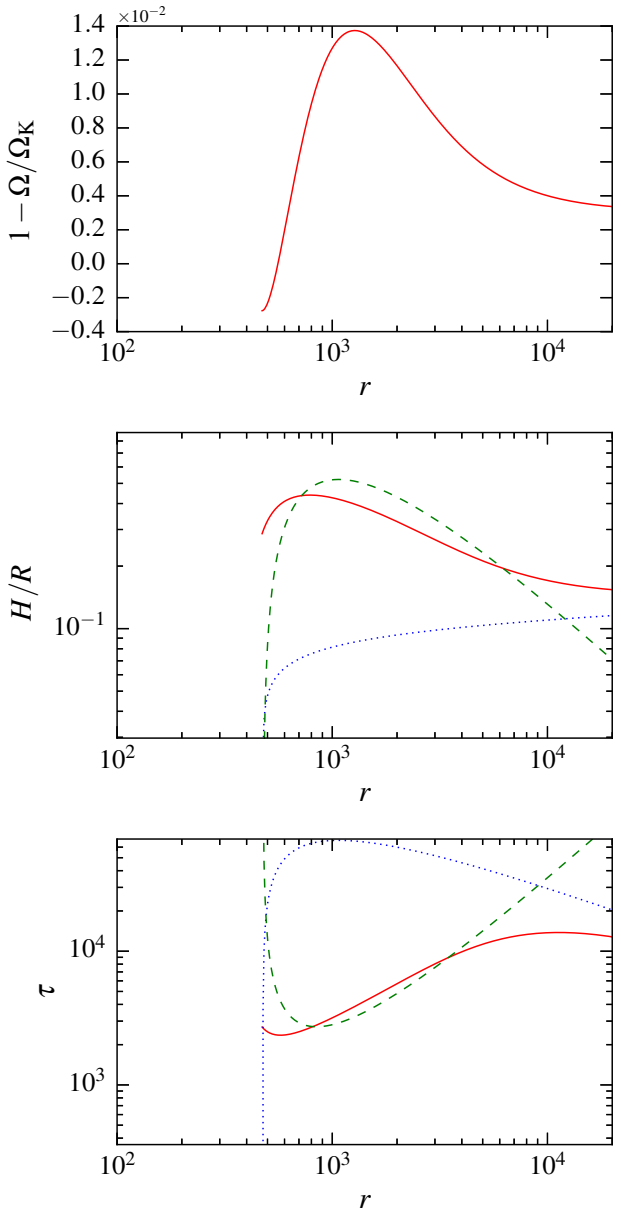

Figure 3.3: Structure of the disc around a NS with magnetic moment $\mu = 10^{30}\,\mathrm{G\,cm^3}$, mass accretion rate $\dot{m} = \dot{M}/\dot{M}_{\rm Edd} = 10$, and spin period 4.87s. The upper panel shows deviations from the Keplerian rotation as a function of the radial coordinate $r = R/R_{\rm g}$. The middle and the bottom panels show the relative disc thickness and the optical depth, respectively. Results for the model described in the Paper II are shown by solid red lines. The standard disc model in radiation-pressure- and gas-pressure-dominated regimes are shown by the dashed green and dotted blue lines, respectively.

significantly. Opacities in the accretion disc are high, hence the effects of irradiation from the accretion column can be written as additional terms in the boundary conditions. First boundary condition acquires an additional term related to the radiation drag and becomes

$$\dot{M}_{\rm in}(\Omega_{\rm in}-\Omega_{\rm NS})R_{\rm in}^2 = k_{\rm t}\frac{\mu^2 H_{\rm in}}{R_{\rm in}^4} + L\frac{\Omega_{\rm in}}{c^2}H_{\rm in}R_{\rm in}. \tag{3.7}$$

In the second boundary condition, a term related to radiation pressure should be added

$$W_{r\phi}^{\rm in} = 2\alpha H_{\rm in}\left(\frac{\mu^2}{8\pi R_{\rm in}^6} + \frac{L}{4\pi R_{\rm in}^2 c}\right). \tag{3.8}$$

The structure of a super-Eddington accretion disc around an accreting magnetized NS is shown in Fig. 3.4.

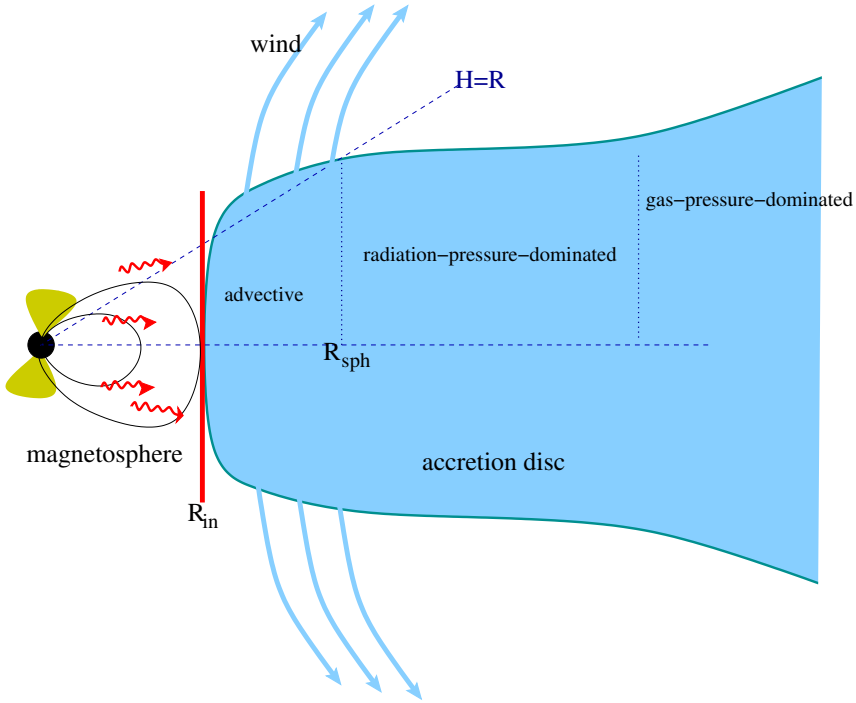

Figure 3.4: Structure of an accretion disc around a ULXP. For very high mass accretion rates, the inner parts of the disc, inside the spherization radius $R_{\rm sph}$ indicated in the sketch, enter the super-Eddington accretion regime. Inside $R_{\rm sph}$, the thin disc model is not applicable. Mass loss in a wind is shown by blue arrows. The accretion column, where most of the energy is released, is shown by yellow cones, and the red wavy lines refer to the radiation of the column that may affect the inner disc pressure balance. The red vertical line marks the effective boundary between the disc and the magnetosphere at the inner radius, see the Paper III.

In reality the radius of the magnetosphere differs from the classical Alfvén radius by a dimensionless factor ξ defined as

$$R_{\rm m} = \xi R_A = \xi \left(\frac{\mu^2}{2\dot{M}\sqrt{2GM}} \right)^{2/7} . \tag{3.9}$$

Analytical models of disc accretion onto magnetized NSs predict the values of the dimensionless coefficient ξ from 0.5 [25, 38, 39] to 1 [75]. MHD simulations for small magnetospheres of young stars and white dwarfs give $\xi \simeq 0.4 - 0.5$. Recent simulations [55] show that ξ is not constant but rather depends on the magnetic field and mass accretion rate. In Papers II and III included in this thesis we confirm this finding using our semi-analytical models. Magnetospheric

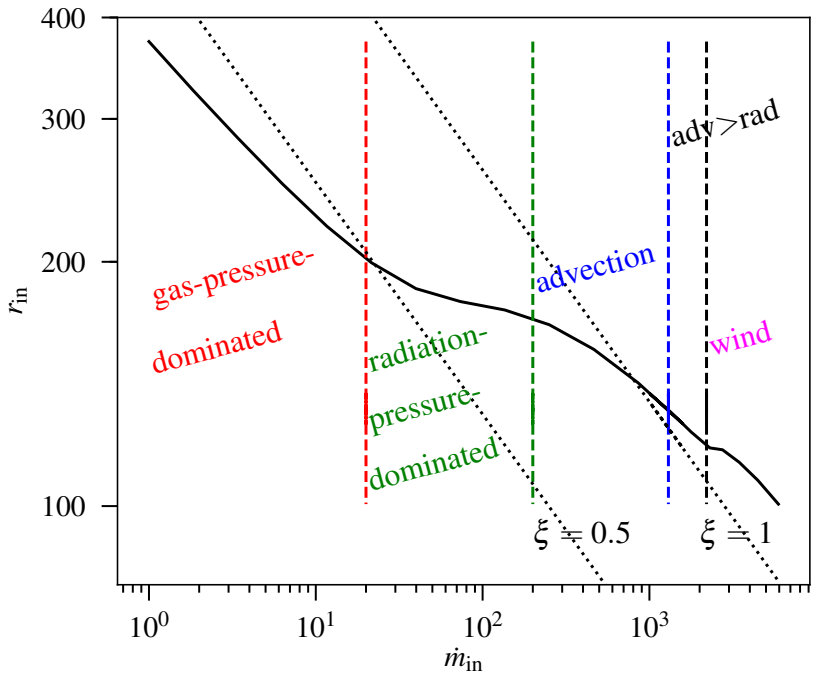

Figure 3.5: Magnetospheric radius in units of $R_{\rm g}$ as a function of the accretion rate for a NS with a magnetic moment of $\mu = 10^{30}$ G cm^3. Parts of the black solid curve with different slopes correspond to the different regimes of accretion near the magnetospheric boundary. Two standard solutions are plotted with the grey dotted lines: $\xi = 0.5$ and $\xi = 1$ (spherically-symmetric case), see Paper III for the details.

radius (in units of gravitational radius $R_{\rm g} = GM/c^2$) dependence on mass accretion rate is shown in Fig. 3.5 for a wide range of accretion rates. The inner regions of the discs in most X-ray pulsars are in the gas-pressure-dominated regime. As the accretion rate increases, radiation

pressure becomes important. For pulsar-scale magnetic fields, $\mu \sim 10^{30}$ G cm^3, this happens at luminosities of a few times $L_{\rm Edd}$, which are quite reachable, for instance, in Be/X-ray binaries during strong outbursts like the recent super-Eddington outburst of SMC X-3 [69, 71]. As we show in Paper II, when the radiation pressure dominates at the inner edge of a sub-critical disc, the magnetospheric radius becomes almost independent of accretion rate

$$R_{\rm in} \approx 170 (\alpha/0.1)^{2/9} (\mu_{30})^{4/9} (M/1.4 M_\odot)^{-10/9} R_{\rm g}, \tag{3.10}$$

where μ_{30} is magnetic moment of the NS in units 10^{30} G cm^3. Thus, provided with a direct measurement of the magnetospheric radius (for example, from quasi-periodic oscillations or from the break in the power density spectrum, see [61] and [47]), we can directly estimate the magnetic moment of the NS, with a weak dependence on the viscosity parameter α.

The inner disc radius is defined mainly by the balance of pressures. The pressure inside the disc is related to its thickness. Thus, the dependence of H/R on $\dot{M}$ is crucial for the behaviour of $R_{\rm in}(\dot{M})$. As the accretion rate increases, advection starts to play important role. The relative thickness of the disc is no more proportional to $\dot{M}$, and the magnetospheric radius again depends on $\dot{M}$. The interplay between wind losses and advection makes the radius dependence on mass accretion rate shallower than the ξ = const approximation historically proposed for spherical accretion but stronger than $R_{\rm in}$ = const.

CHAPTER 4

SUMMARY OF THE ORIGINAL PUBLICATIONS

4.1 Paper I – On the Eddington limit for relativistic accretion discs

In this paper we considered the transition of an accretion disc to the super-Eddington regime. We estimated the critical mass accretion rate taking into account relativistic corrections and found that it is about of factor of two larger than in non-relativistic consideration. Also we found that the non-linear gravity dependence in a realistically thick disc decreases the critical mass accretion rate and estimated the amplitude of the effect. Advection effects work in the opposite direction. We found that including all the effects simultaneously tends to further increase the local Eddington limit, but the efficiency of accretion decreases for the critical mass accretion rate.

4.2 Paper II – Super-Eddington accretion onto a magnetized neutron star

In this paper we proposed a model of an accretion disc interacting with the magnetosphere through a narrow layer near its inner edge. Our model also accounts for radiation pressure from the central source (accretion column). Though the radiation of the disc itself is unlikely to be observed directly, the model allows to find the size of the magnetosphere and, subsequently, to predict equilibrium periods, spin-up rates and possibly other observational properties of both

classical and ultra-luminous X-ray pulsars. We applied this model to the ultraluminous X-ray pulsars M82 X-2 and NGC 7793 P13 and estimated the magnetic moment of the NS in these objects as $\mu = 9 \times 10^{30}$ G cm^3 and $\mu = 7 \times 10^{30}$ G cm^3 respectively. We found that irradiation effects from the column can be important at luminosities $L \geq 10^{40}$ erg s^{-1}.

4.3 Paper III - Super-Eddington accretion discs with advection and outflows around magnetized neutron stars

In this paper we further developed the model described in the Paper II. We took into account the effects of heat advection and mass loss by the wind. This allows to describe the accretion discs in a locally super-Eddington regime. We applied the model to NGC 5907 X-1, known for its very high luminosity, and found the upper limit on its magnetic field $\mu \leq 7.5 \times 10^{31}$/ $\mu \leq 5.5 \times 10^{31}$ G cm^3 without/with irradiation from the accretion column. The model may be applied to a large variety of magnetized neutron stars accreting close to or above their Eddington limits: ultra-luminous X-ray pulsars, Be/X-ray binaries in outbursts, and other systems.

4.4 The author's contribution to the publications

Paper I: On the Eddington limit for relativistic accretion disks

The author of the thesis constructed the basic thin-disc solution and made an equal contribution to the discussion section.

Paper II: Super-Eddington accretion onto a magnetized neutron star

The author wrote the numerical code used to simulate the accretion disc around a neutron star, produced and analyzed the results, and wrote most of the manuscript.

Paper III: Super-Eddington accretion discs with advection and outflows around magnetized neutron stars

The author contributed to the main idea of the paper, wrote a new accretion disc code used for the calculations, and made a significant contribution to the scientific discussion of the results. The author also prepared most of the manuscript.

CHAPTER 5

FUTURE STUDIES

There are two main groups of projects originating from the results and discoveries obtained in my doctoral studies.

5.1 Super-critical accretion onto a black hole

It would be interesting to develop a semi-analytical model of a time-dependent super-critical accretion disc around a black hole in full general relativity taking into account advection and outflows.

In a steady-state slim-disc approximation, this was done by [15]. Even in such a formulation, the problem is complicated both because of the general relativity formalism and due to the singularity at the inner boundary condition related to the transonic nature of the flow. An elegant and potentially rewarding solution of the latter problem is actually to consider a time-dependent problem where the sonic point is no more a singularity but may be tracked during the post-processing stage of the simulation.

Solving this problem will be a step forward in our understanding the physics, variability and dynamics of the objects such as ultra-luminous X-ray sources and rapidly accreting supermassive black holes.

5.2 Super-critical accretion onto a neutron star

The model of super-critical accretion onto a magnetized NS that we present in this thesis is a semi-analytical model. It is important to compare the results with the numerical simulations and observations. The numerical simulations will allow to predict the sizes of the magnetospheres (crucial for magnetic dipole field estimates) and test the thick disc and magnetosphere models. Using the observational data, it will be possible to check the existence of the effects such as the constant magnetosphere size in the radiation-pressure-dominated disc regime predicted in our work.

Another direction of future work is to extend the model of disc accretion onto a magnetized neutron star to the non-stationary case that would allow to calculate the transitions between the accretor and propeller stages, as well as the power spectrum of viscous-timescale variability.

It would be interesting also to consider the spin-down mechanisms in accreting systems with NSs. We know that a NS is spun up by the matter entering the magnetosphere, but the spin-down mechanisms are still poorly understood. It is believed that a NS spins down due to interaction between the magnetic field of a NS and the accretion disc. Recent numerical simulations by [55] have shown that the magnetic field can penetrate the disc only in a narrow band near the inner rim, that is not enough to spin down the NS efficiently. Another possible spin-down mechanism is magnetospheric outflows carrying away the angular momentum from the magnetosphere. This idea can be checked using numerical simulations of magnetospheric accretion.

BIBLIOGRAPHY

[1] P. Abolmasov and A. Chashkina.
On the Eddington limit for relativistic accretion discs.
MNRAS, 454:3432–3444, Dec. 2015.
doi: 10.1093/mnras/stv2229.

[2] P. Abolmasov and N. I. Shakura.
Resolving the inner structure of QSO discs through fold-caustic-crossing events.
MNRAS, 423:676–693, June 2012.
doi: 10.1111/j.1365-2966.2012.20904.x.

[3] M. A. Abramowicz, B. Czerny, J. P. Lasota, and E. Szuszkiewicz.
Slim accretion disks.
ApJ, 332:646–658, Sept. 1988.
doi: 10.1086/166683.

[4] M. A. Abramowicz, X. Chen, S. Kato, J.-P. Lasota, and O. Regev.
Thermal equilibria of accretion disks.
ApJ, 438:L37–L39, Jan. 1995.
doi: 10.1086/187709.

[5] M. A. Abramowicz, X. M. Chen, M. Granath, and J. P. Lasota.
Advection-dominated Accretion Flows around Kerr Black Holes.
ApJ, 471:762, Nov. 1996.
doi: 10.1086/178004.

[6] J. J. Aly.
Electrodynamics of disk accretion onto magnetic neutron star.
A&A, 86:192–197, June 1980.

[7] J. Arons and S. M. Lea.

Accretion onto magnetized neutron stars - Structure and interchange instability of a model magnetosphere.
ApJ, 207:914–936, Aug. 1976.
doi: 10.1086/154562.

[8] L. Arzamasskiy and R. R. Rafikov.
Disk Accretion Driven by Spiral Shocks.
ApJ, 854:84, Feb. 2018.
doi: 10.3847/1538-4357/aaa8e8.

[9] M. Bachetti, F. A. Harrison, D. J. Walton, B. W. Grefenstette, D. Chakrabarty, F. Fürst, D. Barret, A. Beloborodov, S. E. Boggs, F. E. Christensen, W. W. Craig, A. C. Fabian, C. J. Hailey, A. Hornschemeier, V. Kaspi, S. R. Kulkarni, T. Maccarone, J. M. Miller, V. Rana, D. Stern, S. P. Tendulkar, J. Tomsick, N. A. Webb, and W. W. Zhang.
An ultraluminous X-ray source powered by an accreting neutron star.
Nature, 514:202–204, Oct. 2014.
doi: 10.1038/nature13791.

[10] S. A. Balbus.
Enhanced Angular Momentum Transport in Accretion Disks.
ARA&A, 41:555–597, 2003.
doi: 10.1146/annurev.astro.41.081401.155207.

[11] S. A. Balbus and J. F. Hawley.
A powerful local shear instability in weakly magnetized disks. I - Linear analysis. II - Nonlinear evolution.
ApJ, 376:214–233, July 1991.
doi: 10.1086/170270.

[12] M. M. Basko and R. A. Sunyaev.
The limiting luminosity of accreting neutron stars with magnetic fields.
MNRAS, 175:395–417, May 1976.
doi: 10.1093/mnras/175.2.395.

[13] M. C. Begelman.
Super-Eddington Fluxes from Thin Accretion Disks?
ApJ, 568:L97–L100, Apr. 2002.
doi: 10.1086/340457.

[14] M. C. Begelman and D. L. Meier.
Thick accretion disks - Self-similar, supercritical models.
ApJ, 253:873–896, Feb. 1982.
doi: 10.1086/159688.

[15] A. M. Beloborodov.
Super-Eddington accretion discs around Kerr black holes.
MNRAS, 297:739–746, July 1998.
doi: 10.1046/j.1365-8711.1998.01530.x.

[16] A. M. Beloborodov.
Accretion Disk Models.
In J. Poutanen and R. Svensson, editors, *High Energy Processes in Accreting Black Holes*, volume 161 of *Astronomical Society of the Pacific Conference Series*, page 295, Jan. 1999.

[17] H. Bondi.
On spherically symmetrical accretion.
MNRAS, 112:195, 1952.
doi: 10.1093/mnras/112.2.195.

[18] S. Bowyer, E. T. Byram, T. A. Chubb, and H. Friedman.
Cosmic X-ray Sources.
Science, 147:394–398, 1965.
doi: 10.1126/science.147.3656.394.

[19] S. Carpano, F. Haberl, C. Maitra, and G. Vasilopoulos.
Discovery of pulsations from NGC 300 ULX1 and its fast period evolution.
MNRAS, 476:L45–L49, May 2018.
doi: 10.1093/mnrasl/sly030.

[20] A. S. Eddington.
A limiting case in the theory of radiative equilibrium.
MNRAS, 85:408, Mar. 1925.
doi: 10.1093/mnras/85.5.408.

[21] R. Edgar.
A review of Bondi-Hoyle-Lyttleton accretion.
New Astronomy Reviews, 48:843–859, Sep 2004.

doi: 10.1016/j.newar.2004.06.001.

[22] S. N. Fabrika, P. K. Abolmasov, and S. Karpov.
The supercritical accretion disk in SS 433 and ultraluminous X-ray sources.
In V. Karas and G. Matt, editors, *Black Holes from Stars to Galaxies – Across the Range of Masses*, volume 238 of *IAU Symposium*, pages 225–228, Apr 2007.
doi: 10.1017/S1743921307005017.

[23] F. Fürst, D. J. Walton, F. A. Harrison, D. Stern, D. Barret, M. Brightman, A. C. Fabian, B. Grefenstette, K. K. Madsen, M. J. Middleton, J. M. Miller, K. Pottschmidt, A. Ptak, V. Rana, and N. Webb.
Discovery of Coherent Pulsations from the Ultraluminous X-Ray Source NGC 7793 P13.
ApJ, 831(2):L14, Nov 2016.
doi: 10.3847/2041-8205/831/2/L14.

[24] P. Ghosh and F. K. Lamb.
Accretion by rotating magnetic neutron stars. III - Accretion torques and period changes in pulsating X-ray sources.
ApJ, 234:296–316, Nov. 1979.
doi: 10.1086/157498.

[25] P. Ghosh, C. J. Pethick, and F. K. Lamb.
Accretion by rotating magnetic neutron stars. I - Flow of matter inside the magnetosphere and its implications for spin-up and spin-down of the star.
ApJ, 217:578–596, Oct. 1977.
doi: 10.1086/155606.

[26] R. Giacconi, H. Gursky, F. R. Paolini, and B. B. Rossi.
Evidence for x Rays From Sources Outside the Solar System.
Physical Review Letters, 9:439–443, Dec. 1962.
doi: 10.1103/PhysRevLett.9.439.

[27] V. G. Gorbatskii.
Disk-Like Envelopes in Close Binary Systems and Their Effect on Stellar Spectra.
AZh, 41:849, 1964.

[28] A. K. Harding.
The neutron star zoo.
Frontiers of Physics, 8(6):679–692, Dec 2013.

doi: 10.1007/s11467-013-0285-0.

[29] J. W. T. Hessels, S. M. Ransom, I. H. Stairs, P. C. C. Freire, V. M. Kaspi, and F. Camilo.
A Radio Pulsar Spinning at 716 Hz.
Science, 311:1901–1904, Mar. 2006.
doi: 10.1126/science.1123430.

[30] F. Hoyle and R. A. Lyttleton.
On the accretion theory of stellar evolution.
MNRAS, 101:227, 1941.
doi: 10.1093/mnras/101.4.227.

[31] C.-P. Hu, K. L. Li, A. K. H. Kong, C. Y. Ng, and L. C.-C. Lin.
Swift Detection of a 65 Day X-Ray Period from the Ultraluminous Pulsar NGC 7793 P13.
ApJ, 835(1):L9, Jan 2017.
doi: 10.3847/2041-8213/835/1/L9.

[32] S. Ichimaru.
Bimodal behavior of accretion disks - Theory and application to Cygnus X-1 transitions.
ApJ, 214:840–855, June 1977.
doi: 10.1086/155314.

[33] A. F. Illarionov and R. A. Sunyaev.
Why the Number of Galactic X-ray Stars Is so Small?
A&A, 39:185, Feb. 1975.

[34] G. L. Israel, A. Belfiore, L. Stella, P. Esposito, P. Casella, A. De Luca, M. Marelli, A. Papitto, M. Perri, S. Puccetti, G. A. R. Castillo, D. Salvetti, A. Tiengo, L. Zampieri, D. D'Agostino, J. Greiner, F. Haberl, G. Novara, R. Salvaterra, R. Turolla, M. Watson, J. Wilms, and A. Wolter.
An accreting pulsar with extreme properties drives an ultraluminous x-ray source in NGC 5907.
Science, 355:817–819, Feb. 2017.
doi: 10.1126/science.aai8635.

[35] G. L. Israel, A. Papitto, P. Esposito, L. Stella, L. Zampieri, A. Belfiore, G. A. Rodríguez Castillo, A. De Luca, A. Tiengo, F. Haberl, J. Greiner, R. Salvaterra, S. Sandrelli, and G. Lisini.

Discovery of a 0.42-s pulsar in the ultraluminous X-ray source NGC 7793 P13.
MNRAS, 466:L48–L52, Mar. 2017.
doi: 10.1093/mnrasl/slw218.

[36] V. M. Kaspi and M. Kramer.
Radio Pulsars: The Neutron Star Population & Fundamental Physics.
arXiv e-prints, art. arXiv:1602.07738, Feb 2016.

[37] A. R. King, J. E. Pringle, and M. Livio.
Accretion disc viscosity: how big is alpha?
MNRAS, 376:1740–1746, Apr. 2007.
doi: 10.1111/j.1365-2966.2007.11556.x.

[38] W. Kluzniak and S. Rappaport.
Magnetically Torqued Thin Accretion Disks.
ApJ, 671:1990–2005, Dec. 2007.
doi: 10.1086/522954.

[39] A. Koenigl.
Disk accretion onto magnetic T Tauri stars.
ApJ, 370:L39–L43, Mar. 1991.
doi: 10.1086/185972.

[40] E. Körding, H. Falcke, and S. Markoff.
Population X: Are the super-Eddington X-ray sources beamed jets in microblazars or intermediate mass black holes?
A&A, 382:L13–L16, Jan. 2002.
doi: 10.1051/0004-6361:20011776.

[41] L. D. Landau and E. M. Lifshitz.
Fluid mechanics.
1959.

[42] A. Levinson and E. Nakar.
Limits on the growth rate of supermassive black holes at early cosmic epochs.
MNRAS, 473(2):2673–2678, Jan 2018.
doi: 10.1093/mnras/stx2542.

[43] G. V. Lipunova.

Supercritical disk accretion with mass loss.
Astronomy Letters, 25:508–517, Aug. 1999.

[44] D. Lynden-Bell and J. E. Pringle.
The evolution of viscous discs and the origin of the nebular variables.
MNRAS, 168:603–637, Sept. 1974.
doi: 10.1093/mnras/168.3.603.

[45] A. S. Medvedev and J. Poutanen.
Young rotation-powered pulsars as ultraluminous X-ray sources.
MNRAS, 431:2690–2702, May 2013.
doi: 10.1093/mnras/stt369.

[46] J. M. Miller, A. C. Fabian, and M. C. Miller.
A Comparison of Intermediate-Mass Black Hole Candidate Ultraluminous X-Ray Sources and Stellar-Mass Black Holes.
ApJ, 614:L117–L120, Oct. 2004.
doi: 10.1086/425316.

[47] J. Mönkkönen, S. S. Tsygankov, A. A. Mushtukov, V. Doroshenko, V. F. Suleimanov, and J. Poutanen.
Evidence for the radiation-pressure dominated accretion disk in bursting pulsar GRO J1744-28 using timing analysis.
A&A, 626:A106, Jun 2019.
doi: 10.1051/0004-6361/201935507.

[48] R. Narayan and I. Yi.
Advection-dominated accretion: A self-similar solution.
ApJ, 428:L13–L16, June 1994.
doi: 10.1086/187381.

[49] R. Narayan and I. Yi.
Advection-dominated Accretion: Underfed Black Holes and Neutron Stars.
ApJ, 452:710, Oct. 1995.
doi: 10.1086/176343.

[50] I. D. Novikov and K. S. Thorne.
Astrophysics of black holes.

In C. Dewitt and B. S. Dewitt, editors, *Black Holes (Les Astres Occlus)*, pages 343–450, 1973.

[51] B. Paczynski.
Ion viscosity in hot accretion disks.
Acta Astron., 28:253–274, 1978.

[52] D. N. Page and K. S. Thorne.
Disk-Accretion onto a Black Hole. Time-Averaged Structure of Accretion Disk.
ApJ, 191:499–506, July 1974.
doi: 10.1086/152990.

[53] K. Parfrey and A. Tchekhovskoy.
General-relativistic Simulations of Four States of Accretion onto Millisecond Pulsars.
ApJ, 851(2):L34, Dec 2017.
doi: 10.3847/2041-8213/aa9c85.

[54] K. Parfrey, A. Spitkovsky, and A. M. Beloborodov.
Torque Enhancement, Spin Equilibrium, and Jet Power from Disk-Induced Opening of Pulsar Magnetic Fields.
ApJ, 822:33, May 2016.
doi: 10.3847/0004-637X/822/1/33.

[55] K. Parfrey, A. Spitkovsky, and A. M. Beloborodov.
Simulations of the magnetospheres of accreting millisecond pulsars.
MNRAS, 469:3656–3669, Aug 2017.
doi: 10.1093/mnras/stx950.

[56] R. F. Penna, A. Sądowski, A. K. Kulkarni, and R. Narayan.
The Shakura-Sunyaev viscosity prescription with variable α (r).
MNRAS, 428:2255–2274, Jan. 2013.
doi: 10.1093/mnras/sts185.

[57] J. Poutanen, G. Lipunova, S. Fabrika, A. G. Butkevich, and P. Abolmasov.
Supercritically accreting stellar mass black holes as ultraluminous X-ray sources.
MNRAS, 377:1187–1194, May 2007.
doi: 10.1111/j.1365-2966.2007.11668.x.

[58] K. H. Prendergast and G. R. Burbidge.

On the Nature of Some Galactic X-Ray Sources.
ApJ, 151:L83, Feb. 1968.
doi: 10.1086/180148.

[59] J. E. Pringle and M. J. Rees.
Accretion Disc Models for Compact X-Ray Sources.
A&A, 21:1, Oct. 1972.

[60] P. Reig.
Be/X-ray binaries.
Ap&SS, 332(1):1–29, Mar 2011.
doi: 10.1007/s10509-010-0575-8.

[61] M. Revnivtsev, E. Churazov, K. Postnov, and S. Tsygankov.
Quenching of the strong aperiodic accretion disk variability at the magnetospheric boundary.
A&A, 507(3):1211–1215, Dec 2009.
doi: 10.1051/0004-6361/200912317.

[62] H. Riffert and H. Herold.
Relativistic Accretion Disk Structure Revisited.
ApJ, 450:508, Sept. 1995.
doi: 10.1086/176161.

[63] M. M. Romanova, G. V. Ustyugova, A. V. Koldoba, and R. V. E. Lovelace.
MRI-driven accretion on to magnetized stars: global 3D MHD simulations of magnetospheric and boundary layer regimes.
MNRAS, 421:63–77, Mar. 2012.
doi: 10.1111/j.1365-2966.2011.20055.x.

[64] E. T. Scharlemann.
The fate of matter and angular momentum in disk accretion onto a magnetized neutron star.
ApJ, 219:617–628, Jan. 1978.
doi: 10.1086/155823.

[65] N. I. Shakura.
Disk Model of Gas Accretion on a Relativistic Star in a Close Binary System.
AZh, 49:921, Oct. 1972.

[66] N. I. Shakura and R. A. Sunyaev.
Black holes in binary systems. Observational appearance.
A&A, 24:337–355, 1973.

[67] T. Strohmayer and L. Bildsten.
New views of thermonuclear bursts.
In W. Lewin and M. van der Klis, editors, *Compact stellar X-ray sources, Cambridge Astrophysics Series, No. 39*, pages 113–156, Cambridge, Apr. 2006. Cambridge University Press.

[68] C. M. Tan, C. G. Bassa, S. Cooper, T. J. Dijkema, P. Esposito, J. W. T. Hessels, V. I. Kondratiev, M. Kramer, D. Michilli, S. Sanidas, T. W. Shimwell, B. W. Stappers, J. van Leeuwen, I. Cognard, J.-M. Grießmeier, A. Karastergiou, E. F. Keane, C. Sobey, and P. Weltevrede.
LOFAR Discovery of a 23.5 s Radio Pulsar.
ApJ, 866:54, Oct. 2018.
doi: 10.3847/1538-4357/aade88.

[69] L. J. Townsend, J. A. Kennea, M. J. Coe, V. A. McBride, D. A. H. Buckley, P. A. Evans, and A. Udalski.
The 2016 super-Eddington outburst of SMC X-3: X-ray and optical properties and system parameters.
MNRAS, 471:3878–3887, Nov. 2017.
doi: 10.1093/mnras/stx1865.

[70] S. S. Tsygankov, A. A. Mushtukov, V. F. Suleimanov, and J. Poutanen.
Propeller effect in action in the ultraluminous accreting magnetar M82 X-2.
MNRAS, 457:1101–1106, Mar. 2016.
doi: 10.1093/mnras/stw046.

[71] S. S. Tsygankov, V. Doroshenko, A. A. Lutovinov, A. A. Mushtukov, and J. Poutanen.
SMC X-3: the closest ultraluminous X-ray source powered by a neutron star with non-dipole magnetic field.
A&A, 605:A39, Sept. 2017.
doi: 10.1051/0004-6361/201730553.

[72] R. Turolla, S. Zane, and A. L. Watts.
Magnetars: the physics behind observations. A review.

Reports on Progress in Physics, 78(11):116901, Nov. 2015.
doi: 10.1088/0034-4885/78/11/116901.

[73] G. Vasilopoulos, F. Haberl, S. Carpano, and C. Maitra.
NGC 300 ULX1: A test case for accretion torque theory.
A&A, 620:L12, Dec 2018.
doi: 10.1051/0004-6361/201833442.

[74] D. J. Walton, J. C. Gladstone, T. P. Roberts, and A. C. Fabian .
A large catalogue of ultraluminous X-ray source candidates in nearby galaxies.
Astronomische Nachrichten, 332(4):354, May 2011.
doi: 10.1002/asna.201011498.

[75] Y.-M. Wang.
Location of the Inner Radius of a Magnetically Threaded Accretion Disk.
ApJ, 465:L111, July 1996.
doi: 10.1086/310150.

[76] Y. B. Zel'dovich and N. I. Shakura.
X-Ray Emission Accompanying the Accretion of Gas by a Neutron Star.
Soviet Ast., 13:175, Oct. 1969.

UNIVERSITY OF TURKU

Painosalama Oy, Turku , Finland 2019

ISBN 978-951-29-7788-8 (PRINT)
ISBN 978-951-29-7789-5 (PDF)
ISSN 0082-7002 (PRINT) ISSN 2343-3175 (ONLINE)